

Original article

<https://doi.org/10.21285/1814-3520-2021-6-696-707>

## Effect of the sector radius of a workpiece-deforming tool on the stress-strain state in the contact zone with a cylindrical surface

Semen A. Zaides<sup>1</sup>, Quan Minh Ho<sup>2✉</sup>, Nghia Duc Mai<sup>3</sup><sup>1,2</sup> Irkutsk National Research Technical University, Irkutsk, Russia<sup>3</sup> Air Force Officer's college, Nha Trang, Viet Nam<sup>1</sup>zsahaus@mail.ru, <https://orcid.org/0000-0002-7750-7497><sup>2</sup>minhquanho2605@gmail.com, <https://orcid.org/0000-0002-0488-0290><sup>3</sup>nghiamaiduc@gmail.com, <https://orcid.org/0000-0001-6124-3231>

**Abstract.** This paper aims to determine the effect of the sector radius of a workpiece-deforming tool on the stress-strain state in the center of elastoplastic deformation and residual stresses in the hardened zone of the surface layer of cylindrical workpieces. A mathematical model of local loading was constructed using the finite element method and ANSYS software. This model was used to determine the values of temporary and residual stresses and deformations, as well as the depth of plastic zone, depending on the sector radius of the working tool. The simulation results showed that, under the same loading of a cylindrical surface, working tools with different sector radii create different maximum temporary and residual stresses. An assessment of the stress state was carried out for situations when the surface layer of a product is treated by workpiece-deforming tools with a different shape of the working edge. It was shown that, compared to a flat tool, a decrease in the radius of the working sector from 125 to 25 mm leads to an increase in the maximum temporary and residual stresses by 1.2–1.5 times, while the plastic zone depth increases by 1.5–2.4 times. The use of a working tool with a flat surface for hardening a cylindrical workpiece ensures minimal temporary residual stresses, compared to those produced by a working tool with a curved surface. A decrease in the radius of the working sector leads to an increase in temporary residual stresses by 2–7%. The plastic zone depth ranges from 1.65 to 2.55 mm when changing the sector radius of the working tool.

**Key words:** plastic surface deformation, elastic-plastic state, working tool, temporary stress, residual stress, computer modeling

**For citation:** Zaides S. A., Ho Quan Minh, Mai Nghia Duc. Effect of the sector radius of a workpiece-deforming tool on the stress-strain state in the contact zone with a cylindrical surface. *iPolytech Journal*. 2021;25(6):696–707. (In Russ.). <https://doi.org/10.21285/1814-3520-2021-6-696-707>.

### МАШИНОСТРОЕНИЕ И МАШИНОВЕДЕНИЕ

Научная статья

УДК 621.787.4

## Влияние секториального радиуса деформирующего инструмента на напряженно-деформированное состояние в зоне контакта с цилиндрической поверхностью

Семен Азикович Зайдес<sup>1</sup>, Куан Минь Хо<sup>2✉</sup>, Нгиа Дик Май<sup>3</sup><sup>1,2</sup> Иркутский национальный исследовательский технический университет, г. Иркутск, Россия<sup>3</sup> Офицерское училище Военно-Воздушных Сил, г. Начьянг, Вьетнам<sup>1</sup>zsahaus@mail.ru, <https://orcid.org/0000-0002-7750-7497><sup>2</sup>minhquanho2605@gmail.com, <https://orcid.org/0000-0002-0488-0290><sup>3</sup>nghiamaiduc@gmail.com, <https://orcid.org/0000-0001-6124-3231>

**Резюме.** Целью данной работы является определение влияния секториального радиуса рабочего инструмента на напряженно-деформированное состояние в очаге упругопластической деформации и остаточных напряжений в упроченной зоне поверхностного слоя цилиндрических деталей. Для достижения поставленной цели использован метод конечных элементов на основе компьютерной программы ANSYS для построения математической модели локального нагружения, позволяющей определить значения временных, остаточных напряжений и деформаций в зависимости от секториального радиуса рабочего инструмента. Представлены результаты моделирования и определения влияния секториального радиуса рабочего инструмента на напряженно-деформированное состояние поверхностного слоя, включая определение временных и остаточных напряжений, глубины пластической зоны. Полученные результаты компьютерного моделирования подтверждают, что при одинаковых условиях нагружения на цилиндрическую поверхность рабочий инструмент с разными секториальными радиусами создает разные значения максимальных временных и остаточных напряжений. При этом в случае воздействия на цилиндрическую заготовку рабочего инструмента с плоской поверхностью формируются минимальные значения временных остаточных напряжений по сравнению с результатами, полученными при упрочнении криволинейным рабочим инструментом. С уменьшением радиуса рабочего сектора увеличиваются значения временных остаточных напряжений в пределах от 2 до 7%. Глубина пластической зоны при изменении секториального радиуса рабочего инструмента находится в интервале 1,65–2,55 мм.

**Ключевые слова:** поверхностное пластическое деформирование, упругопластическое состояние, рабочий инструмент, временное напряжение, остаточное напряжение, компьютерное моделирование

**Для цитирования:** Зайдес С. А., Хо Куан Минь, Май Нгиа Дик. Влияние секториального радиуса деформирующего инструмента на напряженно-деформированное состояние в зоне контакта с цилиндрической поверхностью // iPolytech Journal. 2021. Т. 25. № 6. С. 696–707. <https://doi.org/10.21285/1814-3520-2021-6-696-707>.

## INTRODUCTION

The technologies of surface plastic deformation (SPD) are widely used to improve the quality and mechanical properties of the surface of machined parts. Hardening treatment by SPD improve such parameters, as wear and corrosion resistance, fatigue strength, tightness, etc. It has been shown that SPD contributes to an increase in the safety margins of products operated under variable loads by 1.5–3 times, and their lifespan by dozens of times [1–4].

However, conventional SPD methods have a number of technological limitations when applied to hardening long-span and low-rigidity cylindrical parts, e.g. shafts and axles. Thus, even under the conditions of low output, it is hard to achieve the specified accuracy of diametral dimensions and the stability of the geometric shape of non-rigid cylindrical parts. Another significant problem in the manufacture of such parts is the distortion of their rectilinear axis [4]. As a result, the products manufactured using SPD either fail to meet the established requirements or demonstrate failures and breakdowns in the course of further operation.

When using SPD for treating non-rigid cylindrical parts, e.g. shafts and axles, it is difficult to obtain the specified quality, since a high radial load from the working tool distorts the shape of the workpiece, failing to provide the stability of mechanical properties along its length. At the

same time, a reduction in the radial load does not always ensure the required quality of the surface layer under an acceptable productivity level.

The described limitations can be overcome by intensifying the stress state in the deformation zone, providing for the required degree of hardening at a constant radial interference. We developed a new design of the working tool for SPD based on a sectorial pendulum, the effect of which on the stress-strain state of the surface layer must be assessed.

In this work, we aim to determine the effect of the sector radius of a workpiece-deforming tool on the stress-strain state in the center of elastoplastic deformation and residual stresses in the hardened zone of the surface layer of cylindrical parts.

## ANALYSIS OF A KNOWN SOLUTION

Specialists at the Irkutsk National Research Technical University developed a new hardening method based on oscillating smoothing of such workpieces as shafts and axles [5]. The method uses the oscillating motion of a deforming tool, which is a flat plate with a spherical radius (fig. 1). Despite a number of distinct advantages, the method has limitations when applied to hardening low-rigidity parts. The reason is a rather high radial load on the workpiece, which leads to its bending. This load can be reduced by reducing

the value of radial interference; however, it will negatively affect the productivity of hardening treatment.

An analysis of the contact between the working tool and the workpiece (fig. 2) showed that, at a constant value of radial interference ( $t$ ), a flat tool has the largest contact zone ( $L$ ), and, consequently, the area of plastic indentation will be the largest. For a working tool of curved geometry, the contact area decreases, increasing the pressure in the contact zone.

## PROBLEM STATEMENT

It seems expedient to investigate the stress-strain state in the contact zone of the workpiece and a workpiece-deforming tool in the form of a circular sector using computer simulation and to determine temporary and residual stresses at different radii of such a tool.

## FINITE ELEMENT MODELING

Computer modeling based on the finite element method (FEM) has been efficiently used to determine the values of temporary and residual

stresses and to analyze the stress-strain state in the deformation zone during hardening by various SPD methods. In this work, FEM was implemented using ANSYS<sup>4</sup> [6], a software application broadly used for these purposes.

When simulating hardening and concurrent processes, either static and dynamic analysis is selected, depending on the complexity of movements of both the deforming tool and the workpiece [7]. In this work, static simulation was applied, since the investigated tool – a circular sector with a spherical radius – does not perform complex movements. This approach allows static data on the processes occurring in the simulated system to be obtained [8]. At the same time, time and its division, the method of constructing network models and their parameters are the main factors for obtaining an accurate assessment of the characteristics of the simulated system [9].

To carry out calculations under static loading, a geometric model was built in the form of a cylinder and a circular sector with a spherical radius on the cylindrical surface (fig. 3).

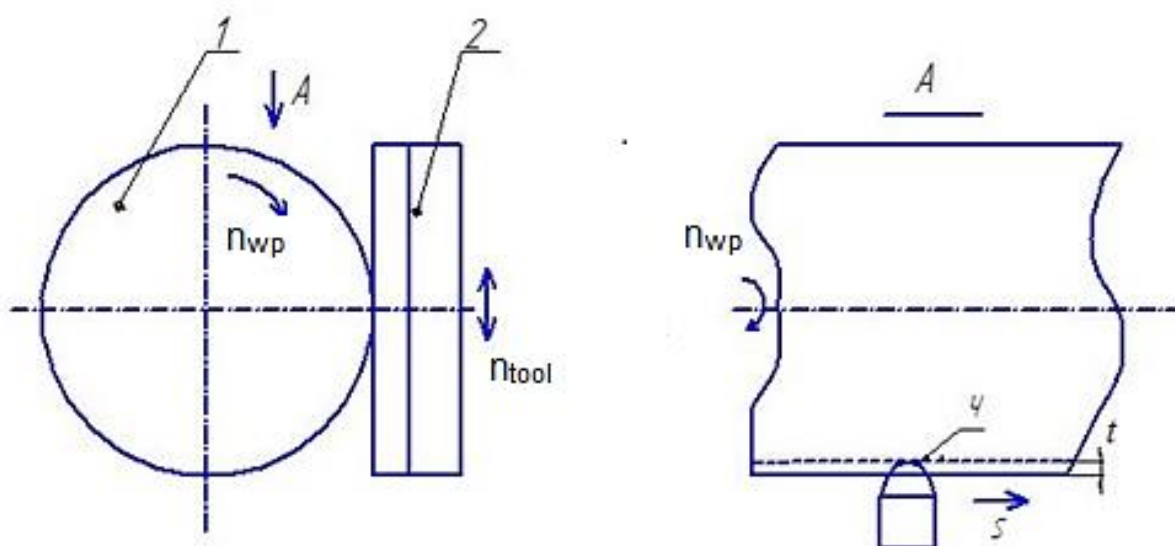


Fig. 1. Oscillatory smoothing diagram [5]: 1 – workpiece; 2 – working tool ( $n_{wp}$  – workpiece rotation frequency, rpm;  $n_{tool}$  – working tool frequency, double stroke per minute)

Рис. 1. Схема осциллирующего выглаживания [5]: 1 – заготовка; 2 – рабочий инструмент ( $n_{заг}$  – частота вращения заготовки, об/мин;  $n_{и}$  – частота инструмента, двойные ходы/мин)

<sup>4</sup>Ваков К. А. ANSYS. User manual. Moscow: DMK Press; 2005, 650 p. / Баков К. А. ANSYS. Справочник пользователя. М.: ДМК Пресс, 2005. 650 с.

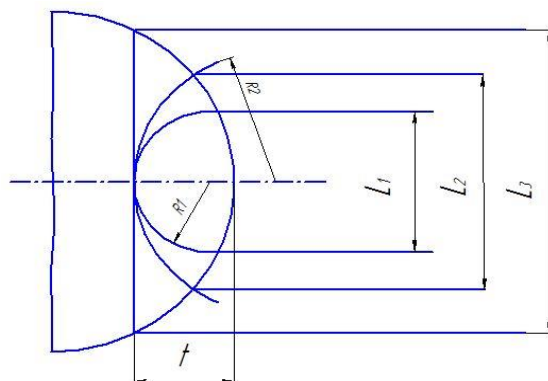


Fig. 2. Diagram of influence of the indenter working part curvature on the contact zone size (R1 – indenter with R1 radius, R2 – indenter with R2 radius)  
 Рис. 2. Схема влияния кривизны рабочей части индентора на размер зоны контакта (R1 – индентор с радиусом R1, R2 – индентор с радиусом R2)

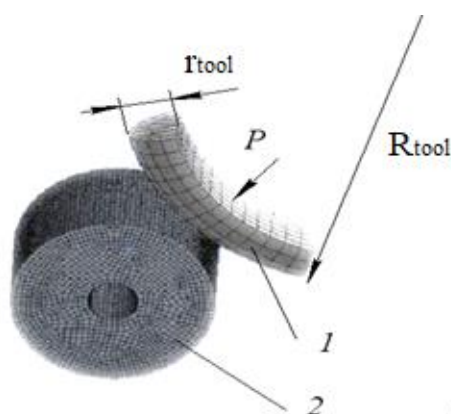


Fig. 3. Finite element model when loading a cylinder with a sectorial tool (P – contact force):  
 1 – circular sector with a rounding radius  $r_{tool}$ ; 2 – cylinder with the diameter  $D_{wp}$   
 Рис. 3. Конечно-элементная модель при нагружении цилиндра секториальным инструментом (P – контактная сила): 1 – круговой сектор с радиусом скругления  $r_u$ ; 2 – цилиндр диаметром  $D_{заг}$

### Main characteristics

Workpiece: a cylinder with a diameter  $D_{wp} = 20$  mm; Workpiece material: steel 45 with elastoplastic and strain-hardening characteristics; modulus of elasticity  $E = 2 \cdot 10^5$  MPa; Poisson's ratio  $\mu = 0.3$ ; bilinear deformation diagram (yield limit  $\sigma_T = 360$  MPa, hardening modulus  $E_T = 1.45 \cdot 10^3$  MPa).

Tool: a circular sector with a spherical radius on the cylindrical surface; alloy VK8; modulus of elasticity  $E = 6 \cdot 10^5$  MPa; Poisson's ratio

$\mu = 0.3$ ; coefficient of friction in the contact zone of the working tool with the workpiece  $f = 0.1$ ; tool working radius  $r_{tool} = 5$  mm.

To assess the **stress** state at different points of a cylindrical specimen, it is necessary to determine the stress intensity (von Mises) and residual stresses along the axes  $O_z$  (axial  $\sigma_z^{res}$ ),  $O_x$  (radial  $\sigma_r^{res}$ ),  $O_y$  (tangential  $\sigma_\phi^{ort}$ ). In this case, when using principal stresses, the stress-strain state of the cylinder according to Von Mises is determined by the stress intensity  $\sigma_i$  <sup>5</sup> [10–12]:

$$\sigma_i = \sqrt{\frac{1}{2} \cdot [(\sigma_z^{res} - \sigma_\phi^{res})^2 + (\sigma_\phi^{res} - \sigma_r^{res})^2 + (\sigma_r^{res} - \sigma_z^{res})^2]}.$$

<sup>5</sup> Bruyaka V. A., Fokin V. G., Kuraeva Ya. V. *Engineering analysis in ANSYS Workbench*. Part 2: learning aid. Samara: Samara Polytech Flagship University; 2013, 149 p. / Бруяка В. А., Фокин В. Г., Кураева Я. В. Инженерный анализ в ANSYS Workbench. Ч. 2: учеб. пособ. Самара: Изд-во СамГТУ, 2013. 149 с.

Table 1. Basic simulation modes

Таблица 1. Базовые режимы моделирования

Workpiece rotation frequency $n_{wp}$ , rpm	Tool rotation frequency $n_{tool}$ , rpm	Negative allowance $t$ , mm	Workpiece diameters $D_{wp}$ , mm	Radius of the working sector $R_{tool}$ , mm	Tool working radius $r_u$ , mm
0	0	0,1	20; 40; 60	25; 50; 75; 100; 125; $\infty$	5

To assess the stress state in the deformation zone and compare the regularity of changes in temporary and residual stresses in the surface layer with an increase in the radius of the working sector, the following basic modes were selected.

## SIMULATION RESULTS

The stress state of a material during SPD is differentiated into temporary and residual stresses. Temporary stresses occur under the action of external forces, while residual stresses occur when these forces are absent. Temporary stresses affect the power characteristics of the process, the depth of the hardened layer, the pressure in the deformation zone, as well as the strength and wear resistance of the workpiece-deforming tool. Residual stresses determine the fatigue strength, fracture processes, wear resistance, corrosion and other operational properties of products [13–16].

Fig. 4 shows the distribution fields of temporary and residual stresses in the cross section of a cylinder at the moment of direct external influence (see fig. 4 a) and in its absence (see fig. 4 b). A working tool with a sector radius  $R_{tool} = 25$  mm acts on the surface of a workpiece with a diameter  $D_{wp} = 20$  mm under loading in basic

modes. Fig. 5 shows the components of temporary and residual stresses along the radius of a workpiece with a diameter  $D_{wp} = 20$  mm.

During SPD under the action of a working tool in the form of a circular sector, residual stresses of compression and residual stresses of tension arise in the surface layer and central zone, respectively. The maximum axial and tangential residual compression stresses are formed on the surface of parts [17, 18]. Radial residual stresses on the surface of the workpiece are equal to zero.

Tab. 2 presents the maximum temporary and residual stresses in the workpiece under the action of a deforming tool in the form of a circular sector with different radii.

On the basis of the data in tab. 2 (with the exception of  $R_{tool} = \infty$ ), dependencies were constructed (fig. 6) for the maximum temporary and residual stresses on the sector radius of the deforming tool for workpieces of various diameters.

## EFFECT OF THE SECTOR RADIUS OF THE WORKING TOOL ( $R_{tool}$ )

The radius of the working sector (sector radius of the working tool) is an important element in the mechanics of deformation and structure

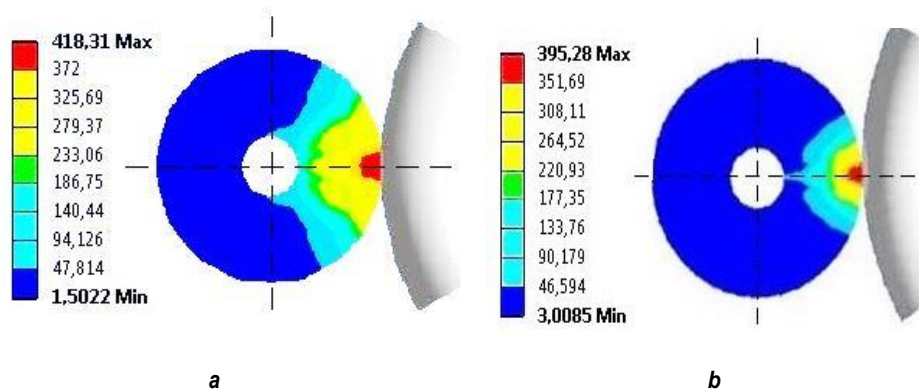


Fig. 4. Distribution zone of intensity of temporary (a) and residual (b) stresses in the cross section of the sample after loading and unloading

Рис. 4. Зона распределения интенсивности временных (a) и остаточных (b) напряжений в поперечном сечении образца после нагружения и разгрузки

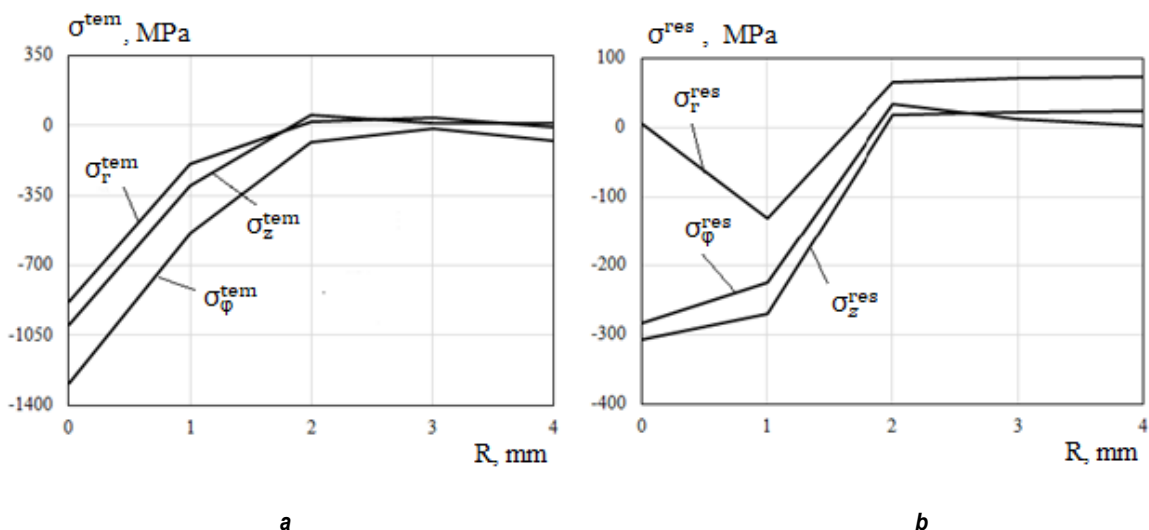


Fig. 5. Distribution of components of temporary (a) and residual (b) stresses along the radius of the sample  
 Рис. 5. Распределение компонент временных (a) и остаточных (b) напряжений вдоль радиуса образца

Table 2. Values of maximum temporary and residual stresses at different values of the working tool sectorial radius  
 Таблица 2. Значения максимальных временных и остаточных напряжений при разных значениях секториального радиуса рабочего инструмента

Maximum stress values, MPa		Working sector radius $R_{tool}$ , mm	25	50	75	100	125	$\infty$
		$D_{wp} = 20$ mm	$\sigma_{max}^{tem}$	418.31	403.91	382.46	367.81	342.71
	$\sigma_{max}^{res}$	395.28	373.46	363.02	346.96	327.47	266.86	
$D_{wp} = 40$ mm	$\sigma_{max}^{tem}$	403.45	393.67	373.78	355.32	331.88	264.98	
	$\sigma_{max}^{res}$	365.22	350.58	342.38	329.76	309.88	228.12	
$D_{wp} = 60$ mm	$\sigma_{max}^{tem}$	385.43	366.11	356.45	342.99	321.55	233.67	
	$\sigma_{max}^{res}$	324.11	303.77	288.55	267.06	255.32	199.85	

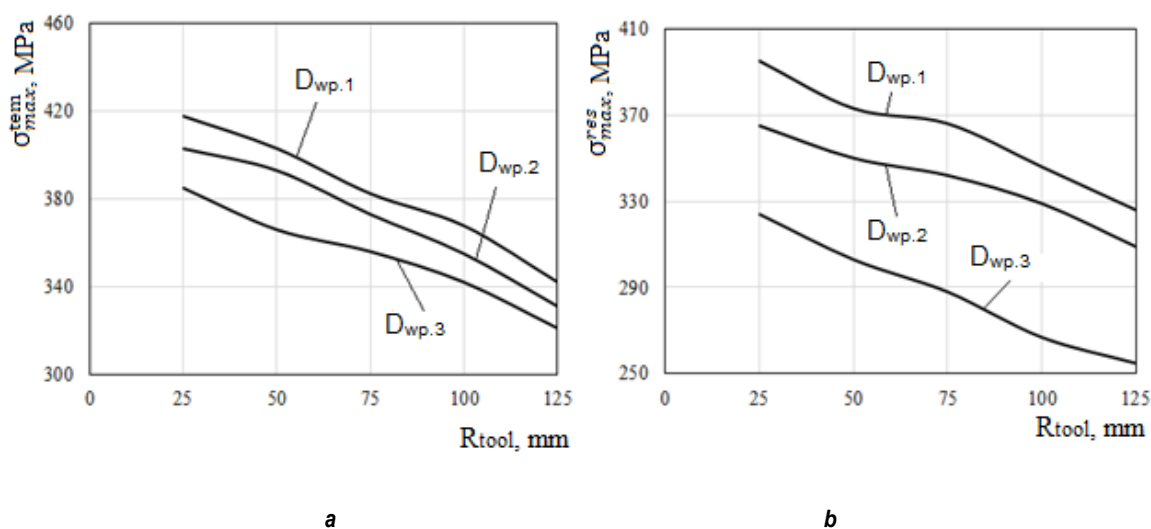


Fig. 6. Influence of the working sector radius on the intensity of maximum temporary (a) and residual (b) stresses:  $D_{wp1} = 20$  mm;  $D_{wp2} = 40$  mm;  $D_{wp3} = 60$  mm

Рис. 6. Влияние радиуса рабочего сектора на интенсивность максимальных временных (a) и остаточных (b) напряжений:  $D_{заг.1} = 20$  мм;  $D_{заг.2} = 40$  мм;  $D_{заг.3} = 60$  мм

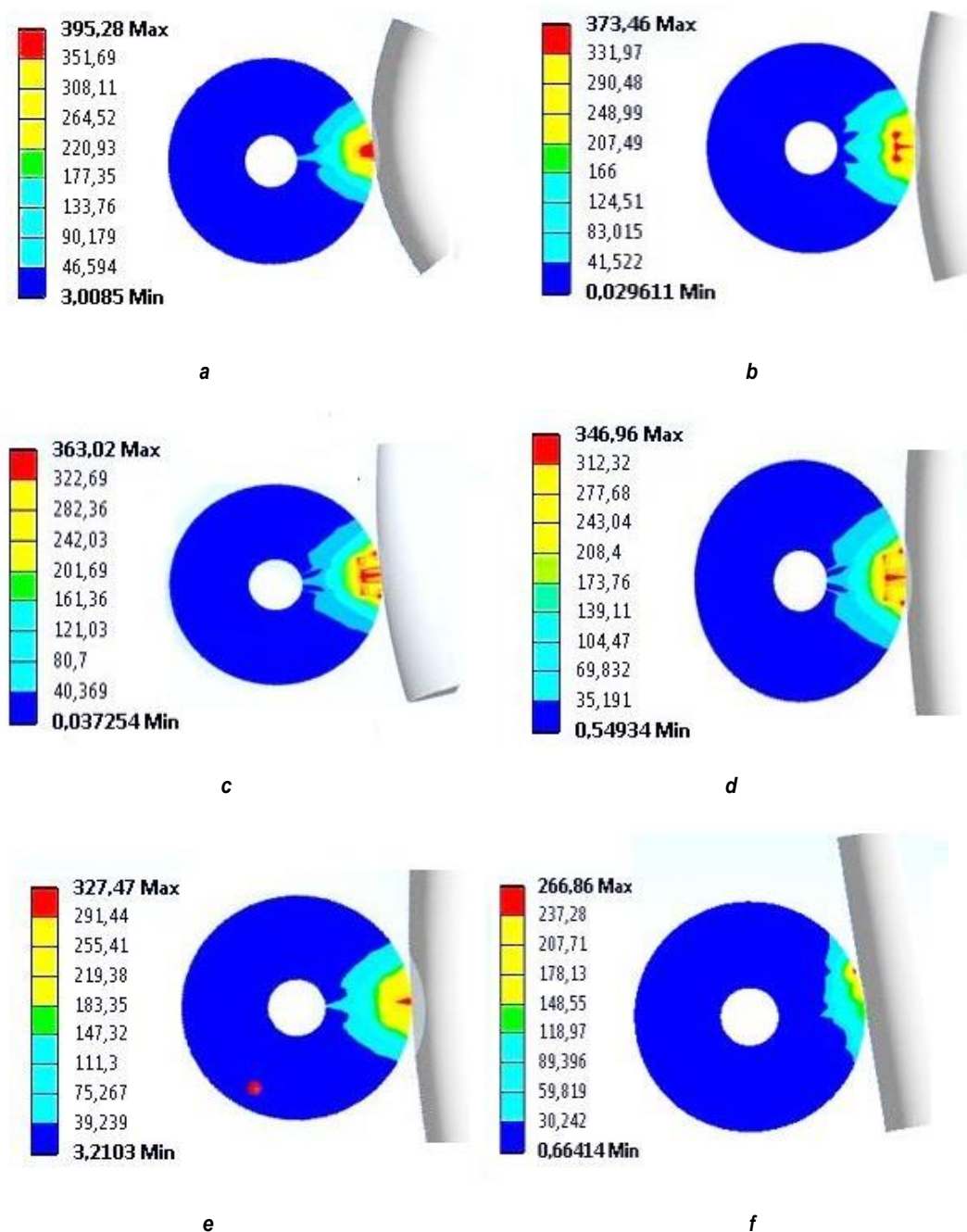


Fig. 7. Distribution fields of maximum residual stress intensity in the cylinder cross section under basic loading conditions :  
a –  $R_{tool} = 25$  mm; b –  $R_{tool} = 50$  mm;

c –  $R_{tool} = 75$  mm; d –  $R_{tool} = 100$  mm; e –  $R_{tool} = 125$  mm; f –  $R_{tool} = \infty$

Рис. 7. Поля распределения интенсивности максимальных остаточных напряжений в поперечном сечении цилиндра при базовых режимах нагружения: а –  $R_u = 25$  мм; б –  $R_u = 50$  мм;

с –  $R_u = 75$  мм; д –  $R_u = 100$  мм; е –  $R_u = 125$  мм; ф –  $R_u = \infty$

formation. This radius should be optimal to ensure the intensification of the deformation process. It can be noted that an increase in the radius of the working sector leads to a decrease in the corresponding temporary and residual stresses (see fig. 6). This can be explained by the fact that an increase in the radius of the

working sector leads to an increase in the contact area. As a result, the stresses are reduced at the same interference values  $t$ .

Fig. 7 shows the distribution fields of the maximum residual stresses depending on the sector radius. Tab. 3 presents the components of the maximum temporary and

residual stresses for a workpiece with a diameter of  $D_{wp} = 20$  mm.

When a flat plate acts as a working tool (see fig. 7 f) on the cylindrical surface of a workpiece, minimal distortion of the microstructure occurs in the contact zone with the formation of the lowest maximum stresses.

With a decrease in the sector radius (see fig. 7 b, c, d, e) of the working tool, residual stresses increase due to a change in the contact area in the deformation zone. As a result of using a working tool with the smallest sectorial radius ( $R_{tool} = 25$  mm), the surface layer of the workpiece undergoes significant plastic deformation (see fig. 7 a) with the accumulation of a large number of distortions. The latter has a significant effect on the quality of hardened products. It should be noted that the area, in which severe plastic deformation occurs, is concentrated in the local zone of contact with the deforming tool, thus

leading to an increase in the maximum stresses.

### SURFACE LAYER DEFORMATION UNDER LOADING BY A WORKING SECTOR TOOL

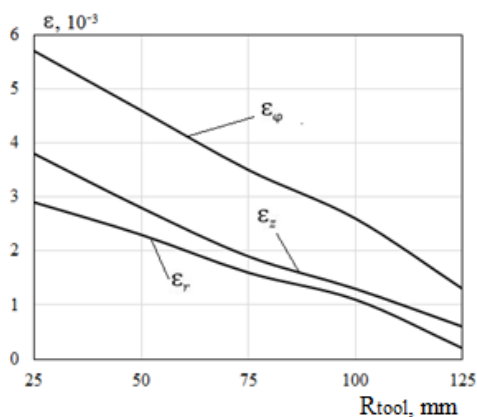
When a cylindrical workpiece is loaded with a working sector tool, the as-formed plastic deformation changes the structure and properties of the surface layer. The strain state is assessed by relative deformations  $\varepsilon$ , which, similar to stresses, are distributed along the three main coordinate axes.

Fig. 8 presents the dependence of relative deformations on the sector radius at a constant penetration depth of the working tool. Obviously, under the same loading, the relative deformation  $\varepsilon$  is inversely proportional to the sector radius of the working tool. It should be noted that the greatest relative deformations under static loading occur in the circumferential (tangential) direction.

**Table 3.** Values of the components of maximum temporary and residual stresses at different radii of the working sector (workpiece diameter  $D_{wp} = 20$  mm)

**Таблица 3.** Значения компонент максимальных временных и остаточных напряжений при разных радиусах рабочего сектора (заготовка диаметром  $D_{зар} = 20$  мм)

$R_{tool}, \text{ mm}$	Temporary stress component, MPa			Residual stress component, MPa		
	$\sigma_{\varphi}^{tem}$	$\sigma_r^{tem}$	$\sigma_z^{tem}$	$\sigma_{\varphi}^{res}$	$\sigma_r^{res}$	$\sigma_z^{res}$
25	-1300.41	-859.69	-914.37	-317.44	-159.44	-328.25
50	-1228.32	-837.65	-870.28	-301.06	-154.58	-319.51
75	-1171.31	-813.93	-846.51	-286.22	-146.06	-301.55
100	-1102.09	-774.51	-825.14	-264.83	-140.95	-288.74
125	-1033.12	-738.31	-807.42	-251.35	-135.32	-261.42
$\infty$	-838.43	-512.45	-754.13	-197.64	-112.432	-183.42



**Fig. 8.** Influence of the working sector radius on the maximum components of relative deformations under interaction with a cylindrical surface

**Рис. 8.** Влияние радиуса рабочего сектора на максимальные компоненты относительных деформаций при взаимодействии с цилиндрической поверхностью

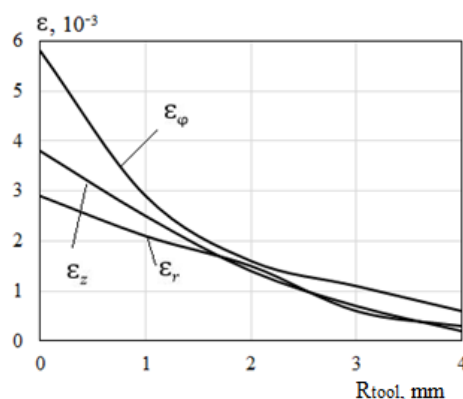


**Fig. 9.** Distribution of plastic deformations along the depth of a cylindrical sample when loaded with a working sector with the radius  $R_{tool} = 25$  mm

**Рис. 9.** Распределение пластических деформаций по глубине цилиндрического образца при нагружении рабочим сектором радиусом  $R_s = 25$  мм

Fig. 9 shows the distribution of three types of deformation in the respective axes along the depth of a cylindrical workpiece under the action of a working sector tool with a radius of  $R_{\text{tool}} = 25$  mm. Here, the relative tangential deformation has the maximum value in the contact zone and decreases towards the center of the workpiece. At the same time, the radial and axial deformations are less significant compared to that in the circumferential (tangential) direction.

## PLASTIC ZONE DEPTH

Plastic zones formed under the action of the working tool serve as a link between the structure and mechanical properties of the treated material, reflecting the peculiarities of its behavior under specific loading conditions [19]. SPD forms plastic zones differing both in shape and size. This has a significant effect not only on the destruction of metallic materials, but also on their resistance to crack propagation [20, 21]. Information on the effective penetration depth of SPD is used for assessing the physical, mechanical and operational properties of hardened parts. Fig. 10 shows the depth of plastic deformation ( $h$ ) under the basic modes of exposure. Tab. 4 describes the depth of hardening at different sector radii of the working tool.

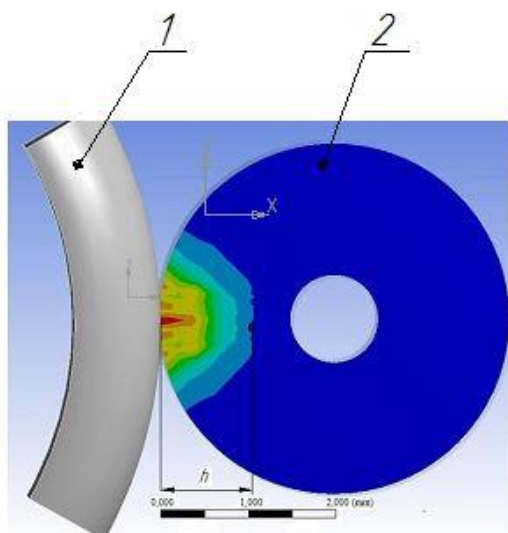


Fig. 10. Distribution fields of plastic deformation in the cross section of the sample at basic loading modes:

1 – working sector; 2 – workpiece

Рис. 10. Поля распределения пластической деформации в поперечном сечении образца при базовых режимах нагружения: 1 – рабочий сектор; 2 – заготовка

**Table 4.** Influence of the working tool sectorial radius on the depth of the plastic zone and the magnitude of the radial stress in the deformation zone

**Таблица 4.** Влияние секториального радиуса рабочего инструмента на глубину пластической зоны и величину радиально напряжения в зоне деформации

$R_u$ , mm	$\sigma_r^{\text{tem}}$ , MPa	$h$ , mm
25	-859.69	2.55
50	-837.65	2.25
75	-813.93	1.95
100	-774.51	1.80
25	-738.31	1.65
$\infty$	-512.45	1.05

The obtained simulation results showed that a decrease in the radius of the working sector increases the depth of the hardened layer. It should be noted that the magnitude of the radial stress in the contact zone is the main factor determining the plastic zone depth. Moreover, when using a flat plate ( $R_{\text{tool}} = \infty$ ), the formed depth of plastic zone has the smallest value compared to that obtained with a circular sector.

Our studies showed that the sector radius of the working tool has a significant effect on the stress-strain state of the surface layer of cylindrical workpieces exposed to SPD, in comparison with hardening with a working tool in the form of a flat plate.

Therefore, our data on the stress-strain state of the surface layer of cylindrical workpieces outline promising directions for the application of SPD for improving the quality of hardened parts, consisting in the use of deforming tools differing from those having a rectilinear shape.

## CONCLUSION

The data on changes in the values of temporary and residual stresses obtained under basic loading conditions using the ANSYS software have allowed us to draw the following conclusions:

1. Under a constant penetration depth of the working tool, the decrease (from 125 to 25 mm) in the sector radius of the working tool leads to an increase (within 4–7%) of the temporary maximum stresses and their constituent components.

2. Upon elimination of the external action of the working tool, residual stresses are formed,

the value of which increases (within 2–6%) with a decrease in the sector radius of the working tool. There is an optimal sector radius (in this study,  $R_{\text{tool}} = 25$  mm), which ensures the formation of the maximum residual stresses that do not exceed the strength limit of the selected material.

3. The inversely proportional dependence of the plastic zone depth on the working sector radius confirms the possibility of a more efficient process of SPD by selecting optimal geometric parameters of the circular sector.

4. An assessment of the stress state of the surface layer under the action of workpiece-deforming tools with a different shape of the working edge was carried out. It was found that, compared to a flat working tool, a decrease in the radius of the working sector from 125 to 25 mm lead to a 1.2–1.5-fold increase in the maximum temporary and residual stresses, and a 1.5–2.4-fold increase in the depth of plastic zone. When using a flat working tool, the maximum temporary and residual stresses are characterized by the smallest values.

### References

1. Odintsov L. G. *Hardening and finishing of parts by surface plastic deformation*. Moscow: Mashinostroenie; 1987, 328 p. (In Russ.).
2. Zaides S. A., Zabrodin V. A., Muratkin V. G. *Surface plastic deformation*. Irkutsk: Irkutsk State Technical University; 2002, 304 p. (In Russ.).
3. Suslov A. G. *Quality of machine part surface layer*. Moscow: Mashinostroenie; 2000, 320 p. (In Russ.).
4. Blyumenshteyn V. Yu., Smelyanskiy V. M. *Mechanics of technological inheritance at the stages of processing and operation of machine parts*. Moscow: Mashinostroenie; 2007, 399 p. (In Russ.).
5. Zaides S. A., Nguen Van Hin', Fam Dak Fyong. *Method of surface plastic deformation*. Patent RF, no. 2657263; 2018. (In Russ.).
6. Bubnov A. S. Technological possibilities of the process of straightening low rigid cylindrical parts by constrained compression. *Vestnik Irkutskogo gosudarstvennogo tekhnicheskogo universiteta = Proceedings of Irkutsk State Technical University*. 2006;4:68-75. (In Russ.).
7. Rayhan S. B., Rahman M. M. Modeling elastic properties of unidirectional composite materials using Ansys Material Designer. *Procedia Structural Integrity*. 2020;28:1892-1900. <https://doi.org/10.1016/j.prostr.2020.11.012>.
8. Ablieieva I., Plyatsuk L., Roi I., Chekh O., Gabbassova S., Zaitseva K., et al. Study of the oil geopermeation patterns: A case study of ANSYS CFX software application for computer modeling. *Journal of Environmental Management*. 2021;287:112347. <https://doi.org/10.1016/j.jenvman.2021.112347>.
9. Bukatiy A. S. Improving the accuracy of manufacturing the engines critical parts by means of static and dynamic modeling. *Izvestiya Samarskogo nauchnogo tsentra Rossiiskoi akademii nauk = Izvestia of Samara Scientific Center of the Russian Academy of Sciences*. 2017;16(6):374-377. (In Russ.).
10. Ivanova L. N. Deformation of shafts and supports of cylindrical gearboxes as a factor influencing transmission loading capacity. *Vestnik mashinostroeniya = Russian Engineering Research*. 2002;11:17-22. (In Russ.).
11. Wu Izhan, Liu Huaiju, Wei Peitang, Lin Qinjie, Zhou Shuangshuang. Effect of shot peening coverage on residual stress and surface roughness of 18CrNiMo7-6 steel. *International Journal of Mechanical Sciences*. 2020;183:105785. <https://doi.org/10.1016/j.ijmecsci.2020.105785>.
12. Li Shen, Kim Do Kyun, Benson S. The influence of residual stress on the ultimate strength of longitudinally compressed stiffened panels // *Ocean Engineering*. 2021;231:108839. <https://doi.org/10.1016/j.oceaneng.2021.108839>.
13. Polyak M. S. *Hardening technology*. In 2 vol., vol. 2. Moscow: Mashinostroenie; 1995, 688 p. (In Russ.).
14. Zaides S. A., Ngo Cao Cuong. Evaluation of stress state in cramped conditions of local loading. *Uprochnyayushchie tekhnologii i pokrytiya = Strengthening Technologies and coatings*. 2016;10:6-9. (In Russ.).
15. Wildemann V. E., Lomakin E. V., Tretyakov M. P. Postcritical deformation of steels in plane stress state. *Mechanics of Solids*. 2014;49(1):18-26. <https://doi.org/10.3103/S0025654414010038>.
16. Smelyanskiy V. M. *Mechanics of part hardening by surface plastic deformation*. Moscow: Mashinostroenie; 2002, 300 p. (In Russ.).
17. Syrigou M., Dow R. S. Strength of steel and aluminium alloy ship plating under combined shear and compression/tension. *Engineering Structures*. 2018;166:128-141.
18. Popov M. E., Aslanyan I. R., Bubnov A. S., Emel'yanov V. N., et al. *Part machining by surface plastic deformation: monograph* / under edition of S. A. Zaides. Irkutsk: Irkutsk State Technical University; 2014, 560 p. (In Russ.).
19. Zhou Changping, Jiang Fengchun, Xu De, Guo Chunhuan, Zhao Chengzhi, Wang Zhenqiang, et al. A calculation model to predict the impact stress field and depth of plastic deformation zone of additive manufactured parts in the process of ultrasonic impact treatment. *Journal of Materials Processing Technology*. 2020;280:116599. <https://doi.org/10.1016/j.jmatprotec.2020.116599>.
20. Ma Chi, Suslov S., Ye Chang, Dong Yalin. Improving plasticity of metallic glass by electropulsing-assisted surface severe plastic deformation. *Materials & Design*. 2019;165:107581.

<https://doi.org/10.1016/j.matdes.2019.107581>.

21. Vulyh N. V., Shchadov I. I. Analysis of the elastic stress-strain state of simulated microroughnesses of hardened surfaces. In: *Zhiznennyj cikl konstrukcionnyh materialov: materialy IV Vserossijskoj nauchno-*

*tekhnicheskoy konferencii s mezhdunarodnym uchastiem = Life cycle of structural materials: materials of IV All-Russian scientific and technical conference with international participation*. Irkutsk: Irkutsk State Technical University; 2014, p. 290-297. (In Russ.).

#### Список источников

1. Одинцов Л. Г. Упрочнение и отделка деталей поверхностным пластическим деформированием. М.: Машиностроение, 1987. 328 с.
2. Зайдес С. А., Забродин В. А., Мураткин В. Г. Поверхностное пластическое деформирование. Иркутск: Изд-во ИГТУ, 2002. 304 с.
3. Суслов А. Г. Качество поверхностного слоя деталей машин. М.: Машиностроение, 2000. 320 с.
4. Блюменштейн В. Ю., Смелянский В. М. Механика технологического наследования на стадиях обработки и эксплуатации деталей машин. М.: Машиностроение, 2007. 399 с.
5. Пат. № 2657263, Российская Федерация, С1, МПК В24В 39/04. Способ поверхностного пластического деформирования / С. А. Зайдес, Ван Хинь Нгуен, Дак Фьонг Фам; заявитель и патентообладатель Федеральное государственное бюджетное образовательное учреждение высшего образования «Иркутский национальный исследовательский технический университет». Заявл. 31.05.2017; опублик. 09.06.2018.
6. Бубнов А. С. Технологические возможности процесса правки маложестких цилиндрических деталей стенным сжатием // Вестник ИргТУ. 2006. № 4. С. 68–75.
7. Rayhan S. B., Rahman M. M. Modeling elastic properties of unidirectional composite materials using Ansys Material Designer // *Procedia Structural Integrity*. 2020. Vol. 28. P. 1892–1900. <https://doi.org/10.1016/j.prostr.2020.11.012>.
8. Ablicieva I., Plyatsuk L., Roi I., Chekh O., Gabbassova S., Zaitseva K., et al. Study of the oil geopermeation patterns: A case study of ANSYS CFX software application for computer modeling // *Journal of Environmental Management*. 2021. Vol. 287. P. 112347. <https://doi.org/10.1016/j.jenvman.2021.112347>.
9. Букатый А. С. Повышение точности изготовления ответственных деталей двигателей средствами статического и динамического моделирования // Известия Самарского научного центра Российской академии наук. 2017. Т. 16. № 6. С. 374–377.
10. Иванова Л. Н. Деформация валов и опор цилиндрических редукторов как фактор влияния на нагрузочную способность передачи // Вестник машиностроения. 2002. № 11. С. 17–22.
11. Wu Izhan, Liu Huaiju, Wei Peitang, Lin Qinjie, Zhou Shuangshuang. Effect of shot peening coverage on residual stress and surface roughness of 18CrNiMo7-6 steel // *International Journal of Mechanical Sciences*. 2020. Vol. 183. P. 105785. <https://doi.org/10.1016/j.ijmecsci.2020.105785>.
12. Li Shen, Kim Do Kyun, Benson S. The influence of residual stress on the ultimate strength of longitudinally compressed stiffened panels // *Ocean Engineering*. 2021. Vol. 231. P. 108839. <https://doi.org/10.1016/j.oceaneng.2021.108839>.
13. Поляк М. С. Технология упрочнения. В 2 т., т. 2. М.: Машиностроение, 1995. 688 с.
14. Зайдес С. А., Нго Као Кыонг. Оценка напряженного состояния при стесненных условиях локального нагружения // Упрочняющие технологии и покрытия. 2016. № 10. С. 6–9.
15. Wildemann V. E., Lomakin E. V., Tretyakov M. P. Postcritical deformation of steels in plane stress state // *Mechanics of Solids*. 2014. Vol. 49. Iss. 1. P. 18–26. <https://doi.org/10.3103/S0025654414010038>.
16. Смелянский В. М. Механика упрочнения деталей поверхностным пластическим деформированием. М.: Машиностроение, 2002. 300 с.
17. Syrigou M., Dow R. S. Strength of steel and aluminium alloy ship plating under combined shear and compression/tension // *Engineering Structures*. 2018. Vol. 166. P. 128–141.
18. Попов М. Е., Асланян И. Р., Бубнов А. С., Емельянов В. Н. [и др.]. Обработка деталей поверхностным пластическим деформированием: монография / под ред. С. А. Зайдеса. Иркутск: Изд-во ИргТУ, 2014. 560 с.
19. Zhou Changping, Jiang Fengchun, Xu De, Guo Chunhuan, Zhao Chengzhi, Wang Zhenqiang, et al. A calculation model to predict the impact stress field and depth of plastic deformation zone of additive manufactured parts in the process of ultrasonic impact treatment // *Journal of Materials Processing Technology*. 2020. Vol. 280. P. 116599. <https://doi.org/10.1016/j.jmatprotec.2020.116599>.
20. Ma Chi, Suslov S., Ye Chang, Dong Yalin. Improving plasticity of metallic glass by electropulsing-assisted surface severe plastic deformation // *Materials & Design*. 2019. Vol. 165. P. 107581. <https://doi.org/10.1016/j.matdes.2019.107581>.
21. Вулых Н. В., Щадов И. И. Анализ упругого напряженно-деформированного состояния моделируемых микронеровностей упрочняемых поверхностей // Жизненный цикл конструкционных материалов: матер. IV Всерос. науч.-техн. конф. с междунар. участием. Иркутск: Изд-во ИГТУ, 2014. С. 290–297.

#### INFORMATION ABOUT THE AUTHORS

**Semen A. Zaides,**

Dr. Sci. (Eng.), Professor,  
Professor of the Department of Materials Science,  
Welding and Additive Technologies,  
Irkutsk National Research Technical University,  
83, Lermontov St., Irkutsk 664074, Russia

**Quan Minh Ho,**

Postgraduate Student,  
Irkutsk National Research Technical University,  
83, Lermontov St., Irkutsk 664074, Russia

**Nghia Duc Mai,**

Cand. Sci. (Eng.),  
Deputy Dean of the Mechanical Engineering Faculty,  
Air Force Officer's college,  
Nha Trang 10000, Viet Nam

**Contribution of the authors**

The authors contributed equally to this article.

**Conflict of interests**

The authors declare no conflicts of interests.

*The final manuscript has been read and approved by all the co-authors.*

**Information about the article**

The article was submitted 01.11.2021; approved after reviewing 06.12.2021; accepted for publication 30.12.2021.

#### ИНФОРМАЦИЯ ОБ АВТОРАХ

**Зайдес Семен Азикович,**

доктор технических наук, профессор,  
профессор кафедры материаловедения, сварочных  
и аддитивных технологий,  
Иркутский национальный исследовательский  
технический университет,  
664074, г. Иркутск, ул. Лермонтова, 83, Россия

**Хо Куан Минь,**

аспирант,  
Иркутский национальный исследовательский  
технический университет,  
664074, г. Иркутск, ул. Лермонтова, 83, Россия

**Май Нгиа Дик,**

кандидат технических наук,  
заместитель декана факультета машиностроения,  
Офицерское училище Военно-Воздушных Сил,  
10000, г. Нячанг, Вьетнам

**Вклад авторов**

Все авторы сделали эквивалентный вклад в подготовку публикации.

**Конфликт интересов**

Авторы заявляют об отсутствии конфликта интересов.

*Все авторы прочитали и одобрили окончательный вариант рукописи.*

**Информация о статье**

Статья поступила в редакцию 01.11.2021; одобрена после рецензирования 06.12.2021; принята к публикации 30.12.2021.